Supporting Online Material

Supplementary Methods

Animals and Surgery. Adult male Sprague-Dawley rats weighing approximately 200 g were maintained according to institutional animal care and use committee (IACUC) guidelines. The relative humidity of the housing room was kept constant at 50±1%. Rats were randomly assigned to sham or injury groups with *n=7* per group. For the behavioral DMS studies, a vehicle group of *n=6* animals and a DMS-treated (0.25 μg/Kg) group of *n=7* animals was used. TNT procedures were performed as previously described [1,2]. In brief, the tibial nerve was exposed in anesthetized animals using blunt-dissection technique and transected distal to the trifurcation of the sciatic nerve. The wound was closed with staples and the animals were allowed to recover on a heating pad. Sham-operated animals were treated identically, except their nerves were not transected. All pain measurements were made by an investigator blinded to the identity of the animal groups, and measured by von Frey filaments to determine 50% paw withdrawal thresholds (PWT) using the method of Dixon where the stimulus is incrementally increased until a positive response is obtained [3]. The 50% PWT was determined as $(10^{[Xf + \kappa\delta]})/10000$, where Xf=the value of the final von Frey filament used in log units, κ=Dixon value for the positive/negative pattern [3], and δ=the mean difference between stimuli in log units.

Metabolomic Analysis. Metabolites were extracted from dissected tissues, harvested astrocytes, or plasma by using cold methanol and acetone as described previously [4,5]. Prior to tissue dissection, animals were deeply anesthetized and transcardially perfused with sterile saline to limit tissue contamination by blood. After sample collection, a volume of 600 μL of cold (-20

ºC) acetone was added to the each sample, vortexed for 30 s, and the sample incubated 1 min in liquid nitrogen. The samples were thawed at room temperature and incubated in liquid nitrogen two more times prior to a 10-min sonication. After 1 h at -20 ºC, the samples were centrifuged at 13,000 rpm for 15 min and the resulting supernatant was stored at -20 ºC. The precipitate was then mixed with 400 μL of methanol/water/formic acid in the ratio of 86.5/12.5/1.0 and sonicated prior to a 1-h incubation at -20 ºC. After centrifugation, the supernatant was collected and transferred to that which was collected after acetone extraction. The solution was dried with a vacuum concentrator (SpeedVac) at room temperature and redissolved in 100 μL of 95% acetonitrile/5% water for liquid chromatography/mass spectrometry analysis. Liquid chromatography was performed by using a reverse-phase C18 column (Zorbax C18, Agilent, 5 μm, 150x0.5 mm diameter column) and a Cogent diamond hydride column (MicroSolv, 4 μm, 150x2.1 mm diameter column) with a flow rate of 20 μl/min and 150 μl/min, respectively. We, and others, have shown previously that this method for metabolite isolation provides quantitatively reliable and efficient extraction of lipid compounds [4-7]. For global profiling, samples were analyzed by using electrospray ionization time-of-flight mass spectrometry (Agilent 6210 TOF) with water/acetonitrile as mobile-phases A/B, each containing 0.1% formic acid. C18 sample analyses used either gradient 1 or gradient 2. Gradient 1 consisted of the following linear changes in mobile-phase B composition with time: 0 min: 10% B, 5 min: 10% B, 10 min: 40% B, 65 min: 98% B, 70 min: 98% B, 75 min: 10% B. Gradient 2 consisted of the following linear changes in mobile-phase B composition with time: 0 min: 10% B, 5 min: 10% B, 10 min: 40% B, 50 min: 98% B, 65 min: 98% B, 66 min: 10% B. Diamond hydride sample analyses started at 90% mobile-phase B with a 20-min linear gradient to 98% mobile-phase A. Sample groups were randomized from run to run, each separated by wash runs, to reduce error

due to instrument variability and possible carryover. The samples were analyzed in both positive- and negative-ion mode. Data were analyzed by using the open-source software XCMS [8]. The XCMS data file for the comparison of the TNT ipsilateral dorsal horn to the sham ipsilateral dorsal horn is available at http://metlin.scripps.edu/data/XCMS_SHAM_TNT/XCMS_SHAM_TNT.pdf. Accurate masses of statistically significant dysregulated features were searched against metabolite databases (e.g., METLIN, HMDB, Kegg's, and Lipid Maps). Metabolite identifications were then made by comparing the retention time and MS/MS fragmentation pattern of the metabolite of interest to that of a standard compound analyzed with identical conditions and collision energy (Agilent 6510 QTOF). All fragmentation data were generated by using a collision energy of 20 volts. Targeted analysis of DMS, S1P, and sphingosine levels were measured by using selective reaction monitoring triple quadrupole mass spectrometry (Agilent 6410 QqQ) and a C18 reverse-phase column with gradient 1 and gradient 2. For DMS, the quantifier ion transition *m/z* 328.3→310.3 and the qualifier 328.3→280.3 was used with a fragmentor voltage of 122 volts and a collision energy of 16 volts and 20 volts respectively. For S1P, the quantifier ion transition of *m/z* 380.3→264.0 and the qualifier 380.3→82.1 transition was used with a fragmentor voltage of 120 volts and a collision energy of 16 volts and 36 volts respectively. For sphingosine, the qualifier ion transition of *m/z* 300.3→282.3 and the qualifier 300.3→55.4 transition was used with a fragmentor voltage of 105 volts and a collision energy of 100 volts and 50 volts respectively. All qualifier and quantifier transitions were optimized from model compounds.

Absolute Quantitation of Metabolites. Concentrations of DMS and S1P were determined by using the standard-addition method. DMS and S1P model compounds were used to make

various concentrations of standard solutions. The ion response for each standard solution was determined by integrating the area of the quantifier transitions listed above for each compound. Standard curves for DMS and S1P were then constructed by plotting ion response versus femtomoles injected into the QqQ mass spectrometer. On the basis of three replicates, the DMS data were fit with a quadratic equation having an R^2 of 0.999 and the S1P data were fit with a quadratic equation having an R^2 of 0.996 (Supplementary Fig 14). Next, metabolites from spinal cord tissue samples were extracted by using the acetone/methanol method detailed above. The protocol yielded 5 μL of solvent extract per 1 mg of tissue. For all samples quantified, 5 μL of solvent extract was injected into the QqQ for analysis. Physiological concentrations of metabolites in tissue were then determined from the ion response by using the standard curves. For DMS and S1P, the ion response for 5 μL of injected sample extract fell within the data points on the standard curve acquired from standards.

Extraction Efficiency. The extraction efficiency of DMS was estimated by spiking known amounts of standard into spinal cord tissues and then performing the metabolite isolation/quantitation protocol described above. Spiked spinal cord tissues were compared to non-spiked contralateral spinal cord tissues from the same animal to account for endogenous levels of DMS. Five independent analyses were performed with different spiked samples. The extraction efficiency of DMS from spinal cord tissue was determined to be 88 ± 4%.

IL-1β and MCP-1 assay. Primary astrocyte cell cultures were prepared from Sprague-Dawley pups 24-48 hrs after birth. Cells were dissociated from the cerebral cortex and plated in

Dulbecco's Modified Eagle's Media (DMEM) containing 10% fetal bovine serum, penicillin, and streptomycin. The culture medium was changed every 2 days until cultures reached confluence, at which point adherent cells were treated with trypsin-EDTA solution and plated on glass coverslips in 35 mm petri dishes at a concentration of 4 $x10^6$ cells/dish. Cells were allowed to adhere and IL-1β or MCP-1 release was measured from 3 biological replicates after incubation with DMS (0.1 μm) for 24 hrs using a rat IL-1β ELISA kit from Invitrogen (Camarillo, CA) or a rat MCP-1 kit from eBioscience (San Diego, CA).

S1P and sphingosine in DMS-treated astrocytes. Immortalized astrocytes were obtained from American Type Culture Collection (CRL-2005) and plated in DMEM containing 10% fetal bovine serum, penicillin, and streptomycin. Cells were incubated in vehicle, 0.1 μM DMS, 1.0 μM DMS, or LPS (10ng/ml) overnight. Cells were harvested by treatment with cold (-20 ºC) methanol and cell scraping. Intracellular metabolites were isolated by using the methods described above. By using the selected reaction monitoring method detailed above, S1P was not detected in any of the intracellular astrocyte extracts or in the astrocyte culture medium. Therefore as an alternative method to monitor the effect of DMS on sphingosine kinase activity, sphingosine levels were measured with the ion transitions above (sphingosine is the substrate of sphingosine kinase). The effect of DMS on intracellular sphingosine levels was not statistically significant (Supplementary Fig 15).

DMS treatment. Chemicals were purchased from Sigma Aldrich (St. Louis, MO) and Cayman Chemical (Ann Arbor, Michigan). Stock solutions of DMS were dissolved in sterile ethanol and

subsequently diluted to concentrations of 0.25 μg/Kg or 1.6 μg/Kg in sterile phosphate-buffer solution (PBS) for injection into animals. Vehicle was ethanol (0.1%) in PBS alone. Animals received a 10 μL intrathecal injection of DMS or vehicle on day 0 of the study and were administered subsequent injections on days 1, 2, 5, 6, and 7. Animals were monitored for the development of mechanical allodynia using von Frey filaments. Tissue was collected on day 7 for immunohistochemical analysis.

Fluorescence Immunohistochemistry. Rats were deeply anesthetized and transcardially perfused with PBS. Brain and spinal cord were removed and frozen in optimal cutting temperature (OCT). Sections of 10-micron thickness were prepared and glial fibrillary acidic protein (GFAP; Millipore, Temecula, CA) was used to identify astrocytes in the tissue. Sections were counterstained with 4',6-diamidino-2-phenylindole (DAPI). Images were taken with a Bio-Rad (Zeiss) Radiance 2100 Rainbow laser scanning confocal microscope (Hercules, CA) and ImageJ (http://rsb.info.nih.gov/ij/) analysis software.

Statistics. Statistical analysis of the metabolomic data was performed by XCMS (employing a two-sample Welch's t-test with unequal variances). Mechanical allodynia is expressed as the mean ± standard deviation (SD). The Student's t-test for unpaired data was used to compare DMS- and vehicle-treated animals as well as DMS- or vehicle-treated astrocyte cultures with the software Prism (where $p<0.05$ was considered statistically significant).

RT-PCR. Dorsal root ganglia were extracted from ipsilateral and contralateral sides of sham-operated and TNT rats post mortem and immersed in RNAlater (Ambion). RNA was extracted from the spinal cord tissue by using a modified acid/phenol protocol and then an RNeasy clean-up protocol (Qiagen) including DNase digestion to remove genomic DNA contamination. RNA quality was assessed by 28S/18S ratio analysis on a 2100 Bioanalyzer (Agilent Technologies) and a A260 Spectrophotometer. RNA samples were reverse transcribed according to the GeneAmp protocol (Applied Biosystems) and expression analysis was carried out by using 10 ng equivalent of cDNA in a 10 ml TaqMan quantitative PCR (Applied Biosystems) reaction. Samples were normalized against 18S ribosomal RNA (rRNA) as an internal positive control, using ΔΔCt analysis (Applied Biosystems). Primers for neutral sphingomyelinase activation associated factor, alkaline ceramidase 1, alkaline ceramidase 2, alkaline ceramidase 3, sphingosine kinase 1, and sphingosine kinase 2 were obtained from Assay on Demand (Applied Biosystems). Primers for receptor S1P1, receptor S1P2, ceramide synthase 1, and acid ceramidase were designed manually by using primer express software. The only statistically significant change detected was in expression of acid ceramidase (Supplemental Fig 11).

Supplementary Results

Identification of DMS. The identification of endogenous DMS in dorsal horn tissue was based on the combination of accurate mass, retention time, and tandem mass spectral data compared to a commercial standard (Fig. 1d, Supplemental Fig 10). To validate that DMS can be resolved on the basis of these experimental parameters from known structural isomers and other compounds within the mass error of the instrument, we considered all database hits in the METLIN, HMDB, KEGG, and LIPID MAPS metabolite libraries within 100 ppm mass accuracy (a value more than

10 times larger than the mass accuracy routinely obtained from the QTOF instrument in which the data were acquired). The database searching resulted in 3 hits for *m/z* of 328.32 that included DMS, sphingosine C-20, and stearoyl ethanolamide. The tandem mass spectra obtained from a stearoyl ethanolamide standard showed a fragmentation pattern that was clearly different from that obtained from the *m/z* 328.32 feature in the research sample (Supplemental Fig 12a). The tandem mass spectra of DMS and sphingosine C-20 both showed fragments at *m/z* 310.31 and 280.30. The intensity of the *m/z* 280.30 fragment, however, was only 16% of the *m/z* 310.31 fragment in sphingosine C-20 whereas it was 45% in DMS and the research sample (Supplemental Fig 12a). Additionally, the sphingosine C-20 standard eluted 3.2 minutes later (using gradient 1) than the DMS standard (Supplementary Fig 12b), which co-eluted with the dysregulated compound detected in the dorsal horn (using both gradients).

Quantitation of DMS. Next, we quantitated the physiological level of naturally occurring DMS in the ipsilateral dorsal horn of TNT animals 21 days after injury. We performed selected reaction monitoring triple quadrupole mass spectrometry where the ion transition *m/z* 328.3→310.3 was used as a quantifier and the ion transition *m/z* 310.3→280.3 was used as a qualifier (Supplementary Fig 10c). The analysis was performed by using gradient 2 (see Supplemental Methods). The ratios between the quantifier and qualifier ion transitions for the DMS standard and the research sample were equivalent, as were the retention times. By using the standard-addition method, we determined that there were 3.5 ± 1.2 fmol of DMS per mg of ipsilateral dorsal horn tissue 21 days after TNT.

Supplementary Table 1. Dysregulated diacylglycerols (DAG) and phosphatidylcholines (PC) in dorsal horn 21 days after TNT.

observed *m/z*	mass	ID	adduct observed	dominant MS/MS fragment	retention time (min)	*p*-value	fold change
634.5405[a]	616.5067	DAG (16:0/20:4)	M + NH_4^+	313.2736, 361.2743	69.1	1.1×10^{-4}	2.7
638.5718[b]	620.5380	DAG (18:0/18:2)	M + NH_4^+	341.3056, 337.2743	74.0	5.8×10^{-4}	3.1
658.5405	640.5067	DAG (16:0/22:6)	M + NH_4^+	313.2743, 385.2743	67.7	3.3×10^{-3}	2.6
660.5561[c]	642.5223	DAG (18:1/20:4)	M + NH_4^+	339.2899, 361.2743	68.9	1.5×10^{-4}	2.7
662.5718	644.5380	DAG (18:0/22:4)	M + NH_4^+	341.3056, 389.3056	69.2	1.1×10^{-4}	2.4
686.5718	668.5380	DAG (18:0/22:6)	M + NH_4^+	341.3056, 385.2743	71.1	3.4×10^{-4}	3.0
730.5405[d]	712.5068	DAG (22:6/22:6)	M + NH_4^+	385.2743	64.1	3.5×10^{-6}	2.6
552.4023	551.3951	PC ($C_{28}H_{58}NO_7P$)	N/A (M + H^+)	187.0730	37.2	5.6×10^{-4}	5.0
782.5694[a]	781.5622	PC ($C_{44}H_{80}NO_8P$)	N/A (M + H^+)	187.0730	60.8	1.0×10^{-2}	3.2
786.6007[b]	785.5935	PC ($C_{44}H_{84}NO_8P$)	N/A (M + H^+)	187.0730	43.3	1.0×10^{-2}	2.8
830.5670[c]	807.5778	PC ($C_{46}H_{82}NO_8P$)	M + Na^+	187.0730	68.6	3.0×10^{-3}	3.4
832.6790[e]	831.6717	PC ($C_{47}H_{94}NO_8P$)	N/A (M + H^+)	187.0730	63.5	3.3×10^{-3}	63.5

[a] accurate masses and fragments consistent with same acyl chains
[b] accurate masses and fragments consistent with same acyl chains
[c] accurate masses and fragments consistent with same acyl chains
[d] Fragmentation pattern shown in Supplementary Fig 5
[e] Fragmentation pattern shown in Supplementary Fig 4

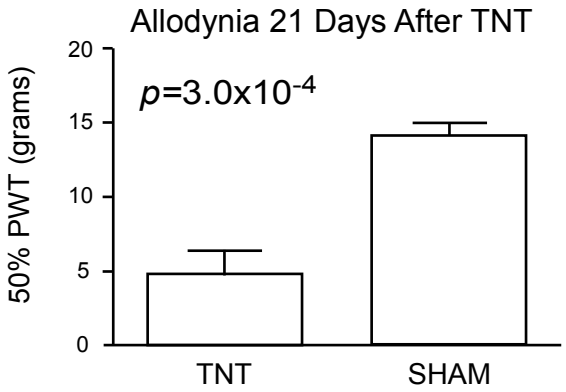

Supplementary Figure 1. Measurement of mechanical allodynia in sham-operated and TNT animals 21 days after tibial nerve transection. Data are expressed as 50% paw withdrawal threshold (PWT) of mean ±SD (*n=10* animals per group, $p=3.0x10^{-4}$ by a Student's t-test for unpaired data). The tibial nerve was transected and the dorsal horn dissected 21 days after surgery for metabolomic analysis.

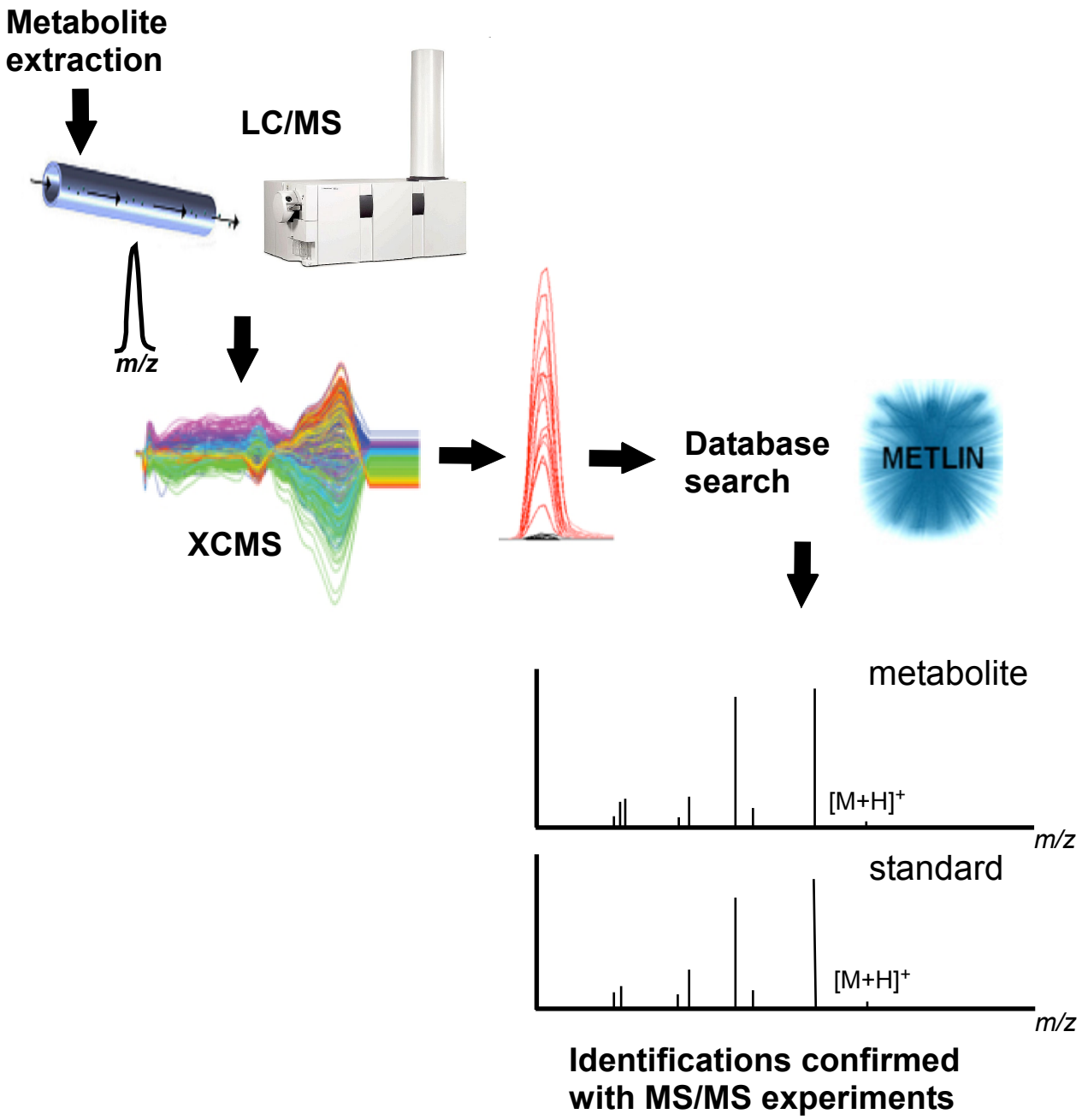

Supplementary Figure 2. Workflow for untargeted metabolomic analysis of neuropathic pain samples. Samples were first analyzed by liquid chromatography/electrospray ionization time-of flight mass spectrometry. Data were processed by using an open-source metabolomic software program called XCMS. The accurate masses of dysregulated features were then searched against metabolite databases (e.g., METLIN). Putative identifications were confirmed by comparing the tandem mass spectra and retention time of model compounds to that of the research sample.

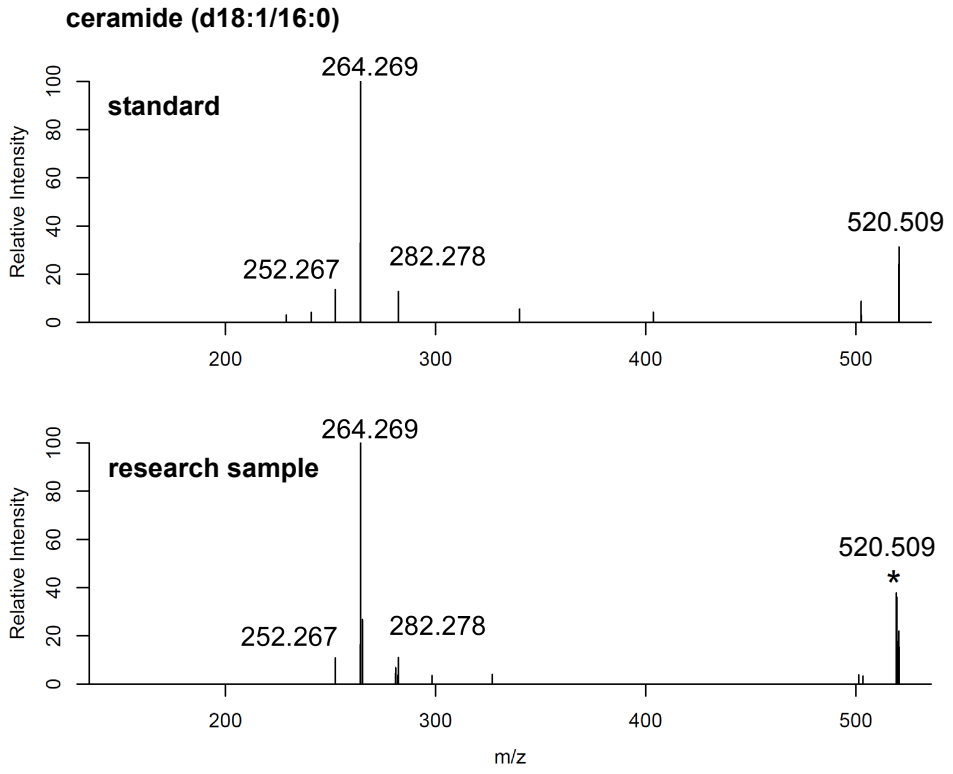

Supplementary Figure 3. Tandem mass spectra for ceramide (d18:1/16:0). The fragments and their relative intensities for the model compound are consistent with the identification of ceramide (d18:1/16:0) in the dorsal horn.

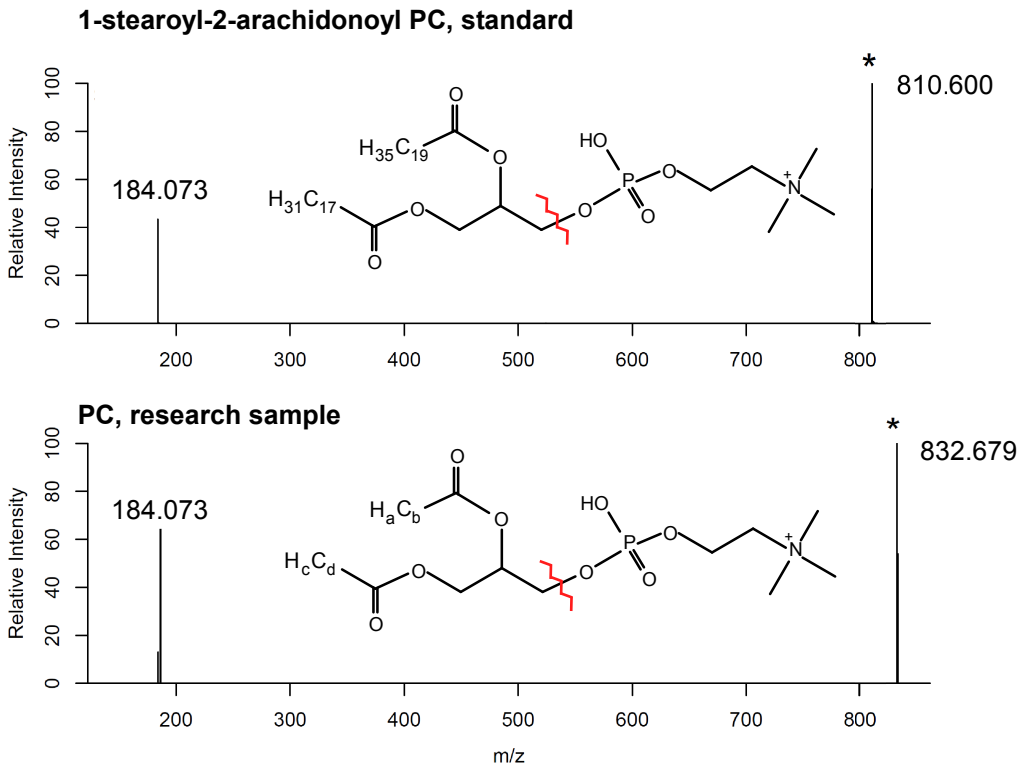

Supplementary Figure 4. Tandem mass spectra for phosphatidylcholine. Phosphatidylcholines produce a characteristic fragment at *m/z* 184.073 as shown for the representative standard that was used for identification. The red dagger indicates the structural prediction of the fragment from the METLIN database.

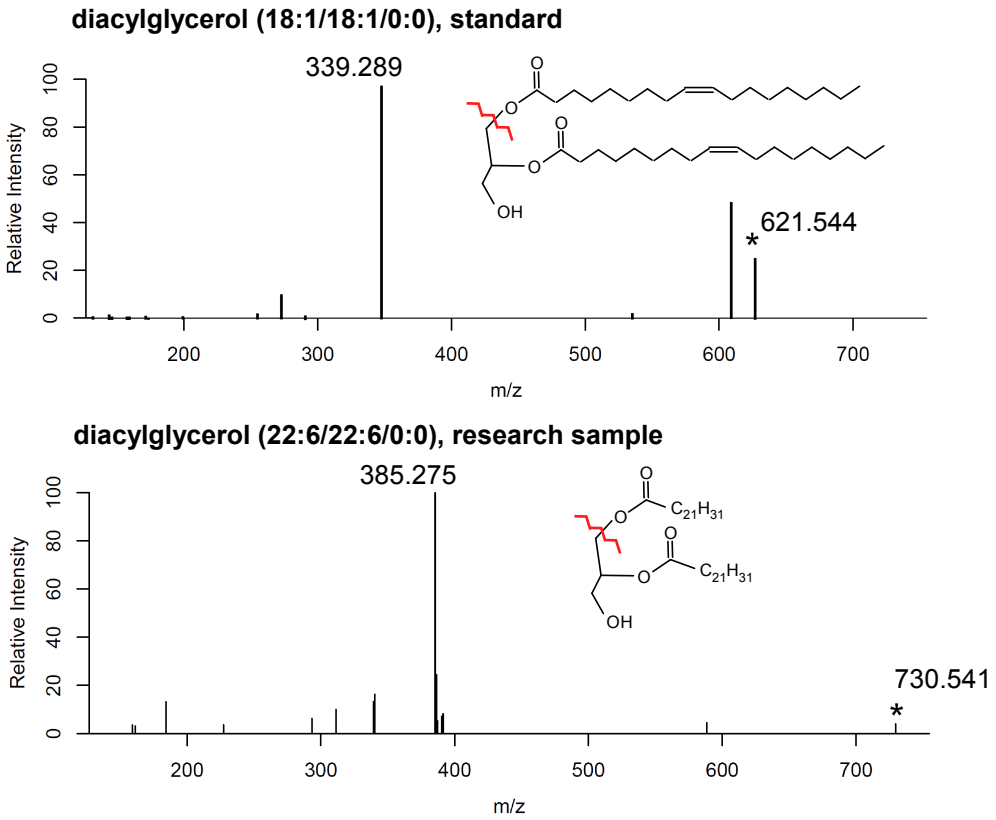

Supplementary Figure 5. Tandem mass spectra for diacylglycerols. Diacylglycerols have a characteristic fragmentation pattern as shown for the representative standard that was used for identification. Each acyl chain produces a fragment as indicated by the red daggers in the structures provided. For the examples shown, because the acyl chains have the same *m/z* values, there is only 1 major fragment.

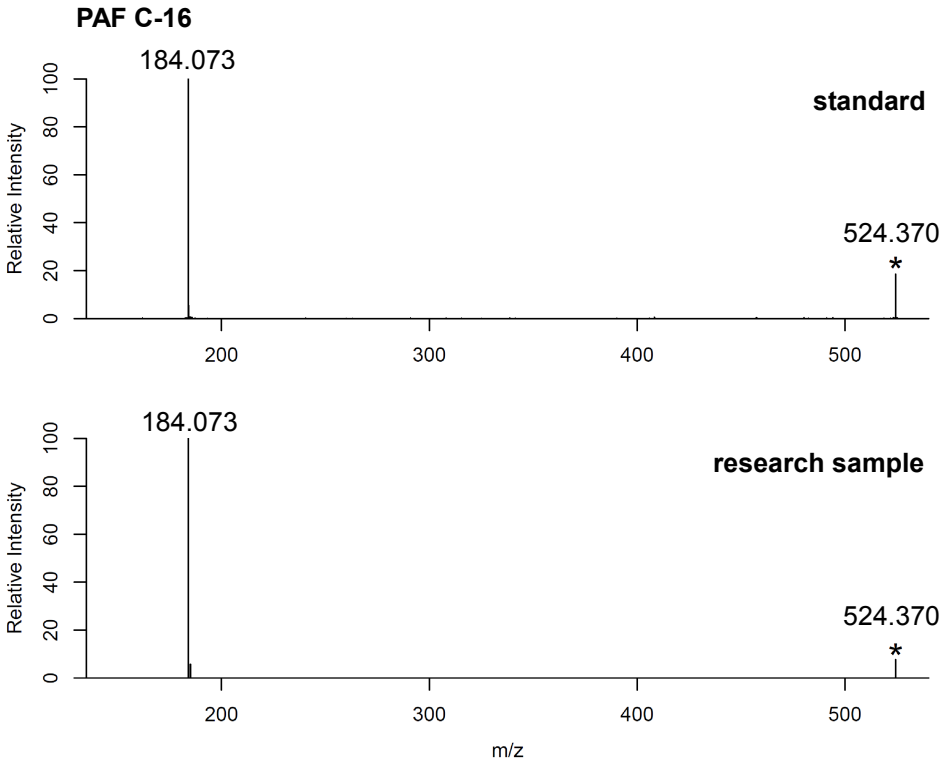

Supplementary Figure 6. Tandem mass spectra for PAF C-16. Fragmentation of PAF C-16 produces a major fragment at *m/z* 184.073 that was used for identification.

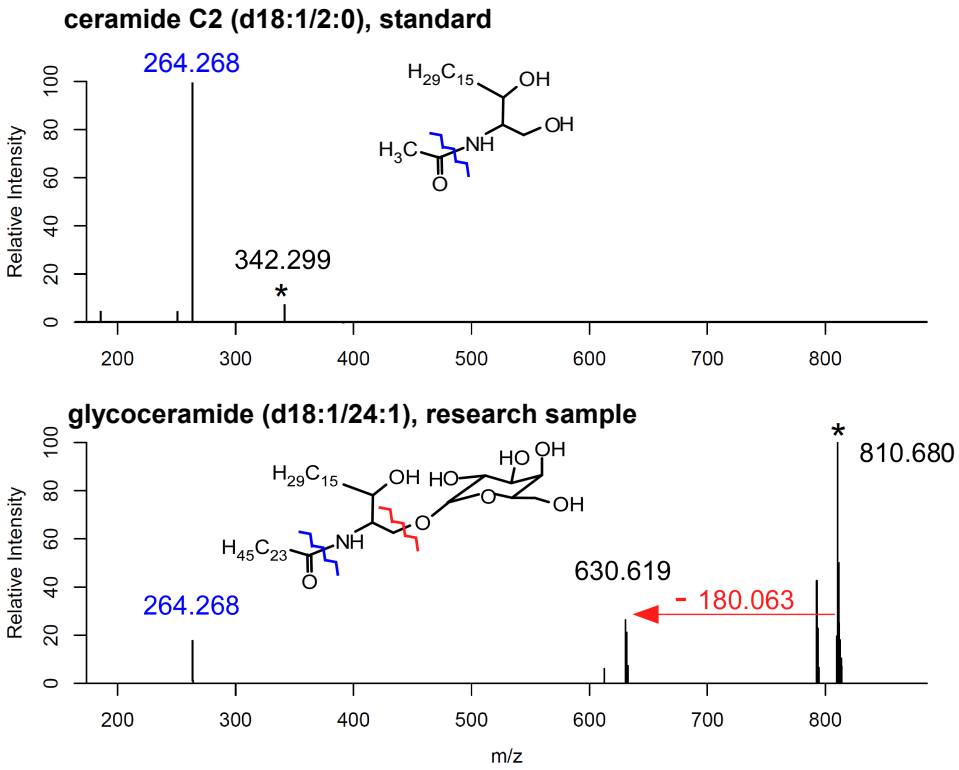

Supplementary Figure 7. Tandem mass spectra for ceramide species with a d18:1 chain produce a characteristic fragment at *m/z* 264.268 as shown for the representative standard ceramide C2 (d18:1/2:0). Monohexosylceramide metabolites have a characteristic neutral loss corresponding to the loss of sugar (*m/z* 180.063) as shown by the red dagger. The combination of these data, in addition to accurate mass and retention time, was used to identify monohexosylceramide (d18:1/24:1) in the dorsal horn. Based on our mass spectrometric methods, it is not possible to distinguish glucosylceramide (d18:1/24:1) from galactosylceramide (d18:1/24:1).

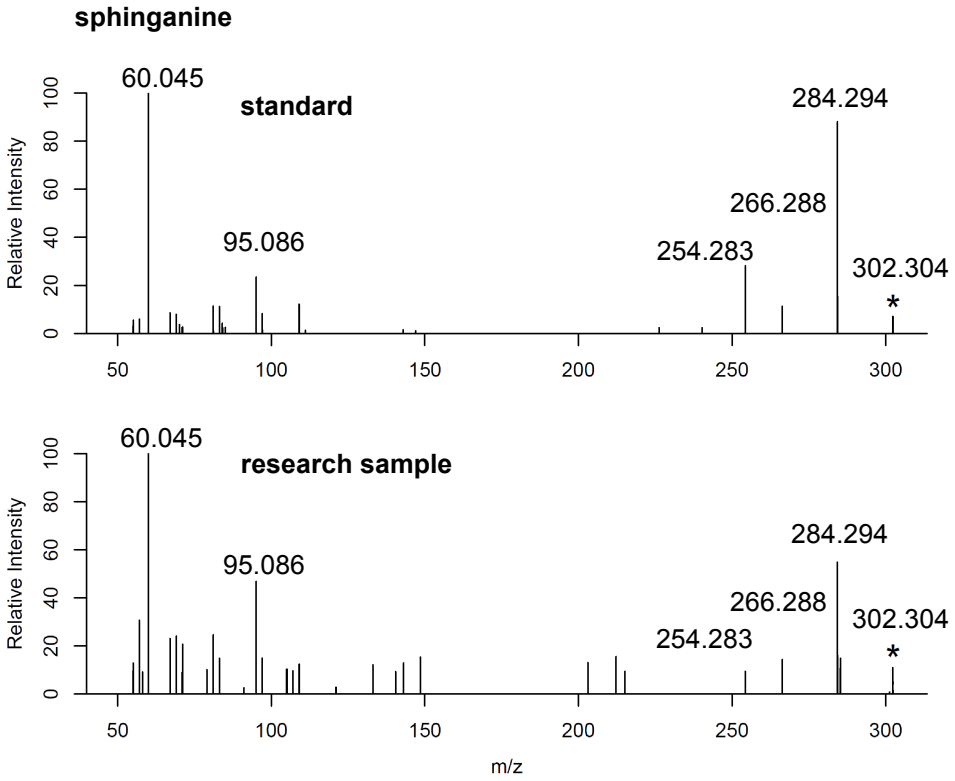

Supplementary Figure 8. Tandem mass spectra for sphinganine. The fragments and their relative intensities for the model compound are consistent with the identification of sphinganine in the dorsal horn.

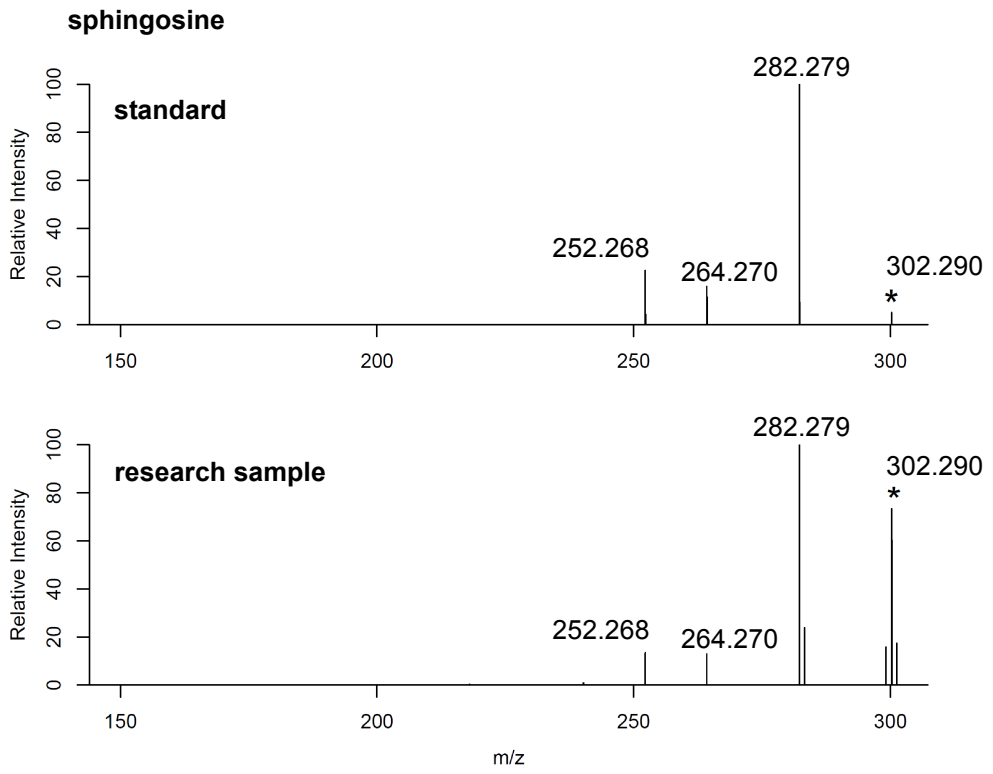

Supplementary Figure 9. Tandem mass spectra for sphingosine. The fragments and their relative intensities for the model compound are consistent with the identification of sphingosine in the dorsal horn.

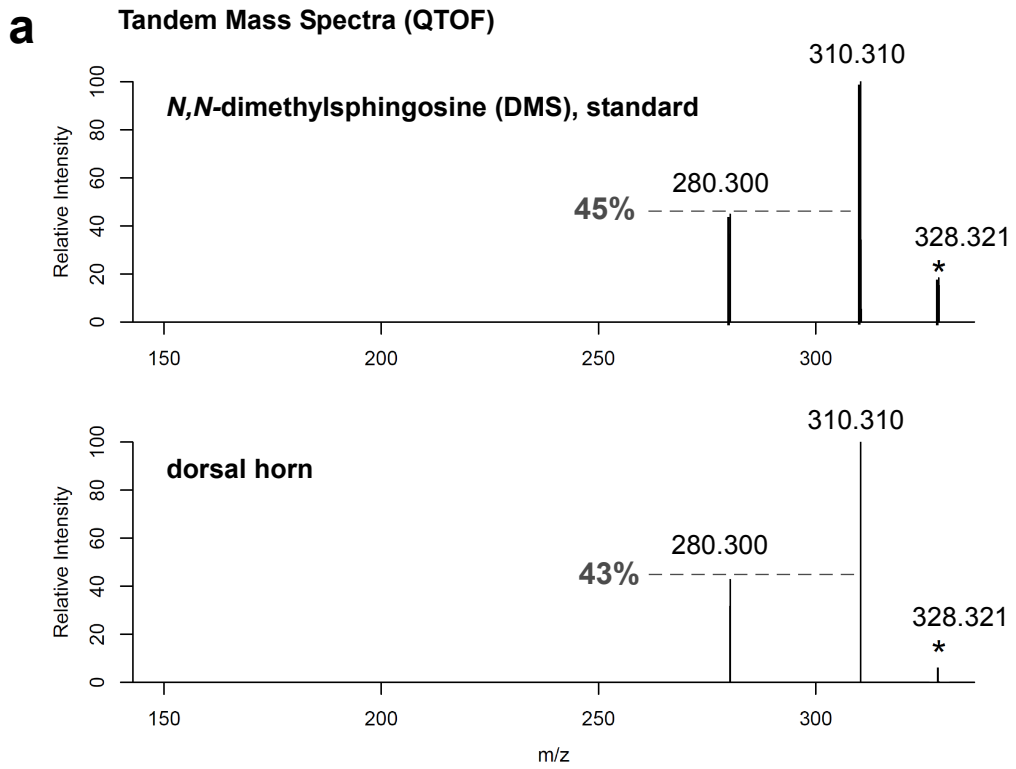
a
Tandem Mass Spectra (QTOF)
N,N-dimethylsphingosine (DMS), standard
310.310
280.300
45%
328.321
*
Relative Intensity
0
20
40
60
80
100
150
200
250
300
dorsal horn
310.310
280.300
43%
328.321
*
Relative Intensity
m/z

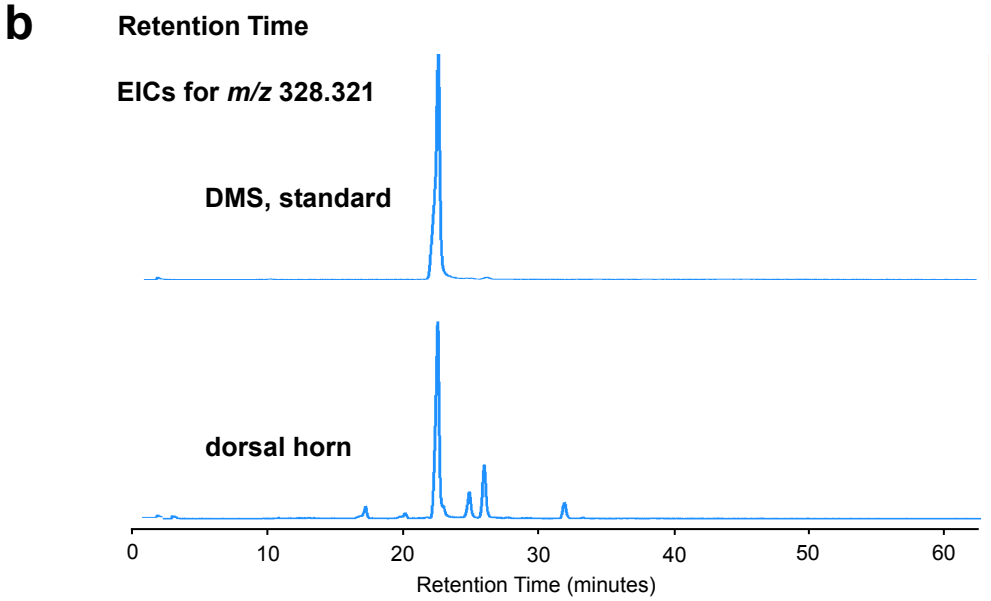
b
Retention Time
EICs for m/z 328.321
DMS, standard
dorsal horn
0
10
20
30
40
50
60
Retention Time (minutes)

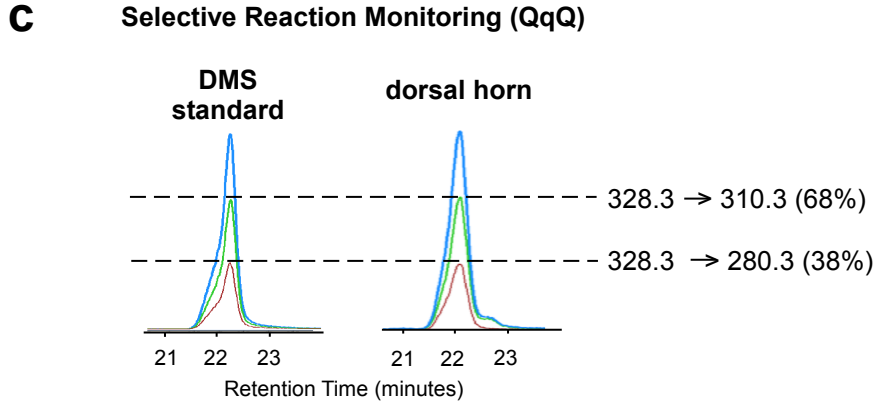
c
Selective Reaction Monitoring (QqQ)
DMS standard
dorsal horn
328.3 → 310.3 (68%)
328.3 → 280.3 (38%)
21
22
23
21
22
23
Retention Time (minutes)

Supplementary Figure 10. Identification of *N,N*-dimethylsphingosine (DMS). (a) The tandem mass spectra of the DMS standard is characterized by 2 fragments at *m/z* 310.310 and 280.300. The relative intensity of the 280.300 fragment is 45% of the intensity of the 310.310 fragment. The same 2 characteristic fragments were detected in the research sample with a comparable ratio of intensities. (b) The DMS standard elutes with the same retention time as the dysregulated feature with *m/z* 328.321 in the dorsal horn (22.3 min for gradient 2 as shown here, 26.0 min for gradient 1 as shown in Supplementary Figure 12). (c) Selective reaction monitoring by triple quadrupole mass spectrometry of the ion transitions 328.3→310.3 and 328.3→280.3 show consistent ratios in the DMS standard and dorsal horn.

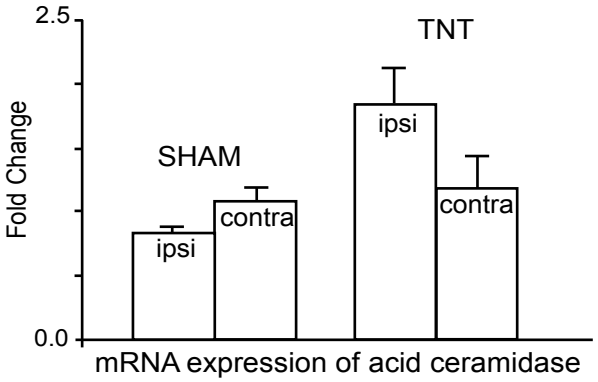

Supplementary Figure 11. RT PCR for acid ceramidase expression in the dorsal root ganglia. Dorsal root ganglia were taken 21 days after TNT and RNA was extracted for analysis of acid ceramidase expression. Acid ceramidase expression is up-regulated by 2.3 fold in the ipsilateral dorsal root ganglia of TNT animals compared to the contralateral dorsal root ganglia and sham animals (p=3.4x10^{-3}).

a **Tandem Mass Spectra (QTOF)**

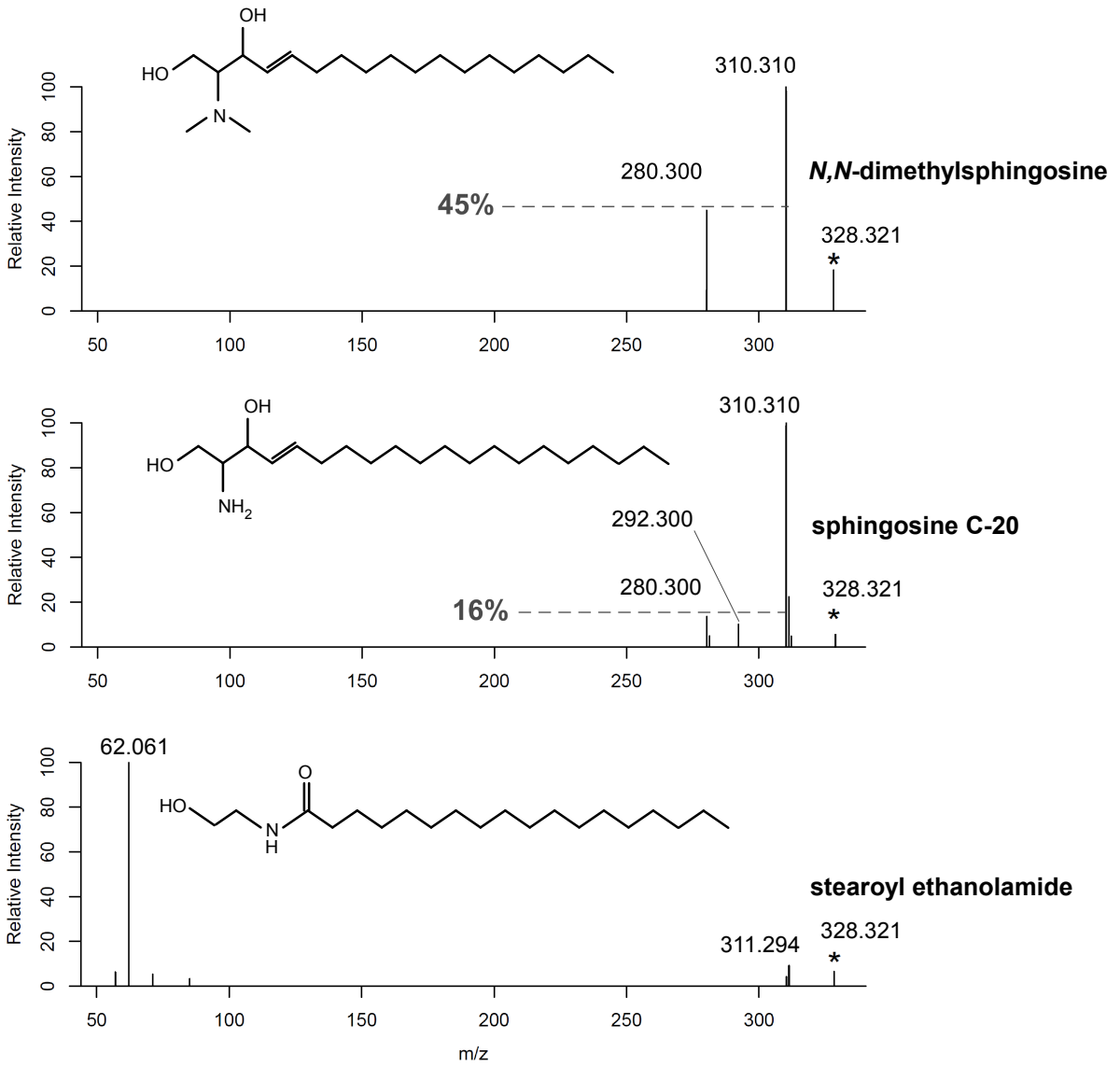

b **Retention Time**

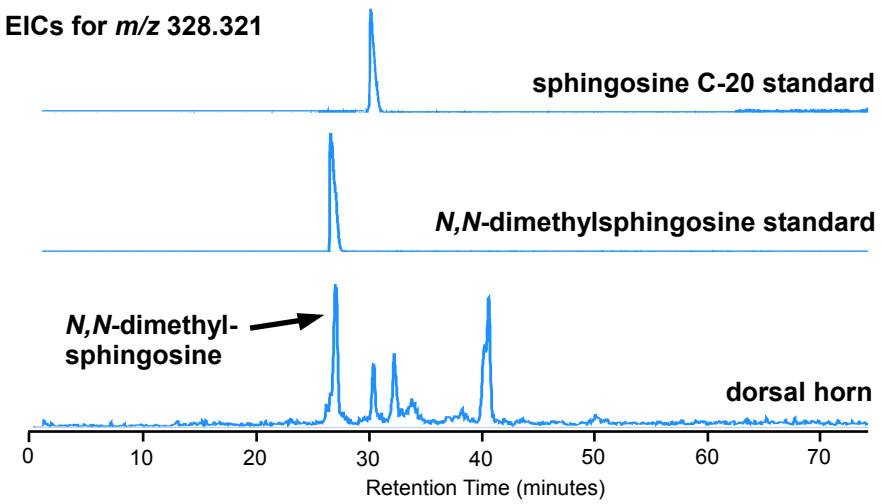

Supplementary Figure 12. Distinguishing DMS from structural isomers in the METLIN, HMDB, Kegg's, and Lipid Maps databases. (a) Tandem mass spectra for DMS, sphingosine C-20, and stearoyl ethanolamide. Although DMS and sphingosine C-20 produce fragments at *m/z* 310.310 and 280.300, the ratio of their relative intensities is different with the *m/z* 280.300 fragment being substantially reduced for sphingosine C-20. Additionally, sphingosine C-20 produces a fragment at *m/z* 292.300 that is absent for DMS. The tandem mass spectrum for stearoyl ethanolamide does not share any common fragments with *m/z* 328.321 from the research sample. (b) Extracted ion chromatograms (EICs) of *m/z* 328.321. DMS and sphingosine C-20 have unique retention times on a reverse-phase C18 column. By using gradient 1, sphingosine C-20 elutes 3.2 min later than the DMS standard. The DMS standard elutes at the same time as the *m/z* 328.321 ion determined to be dysregulated in the research sample.

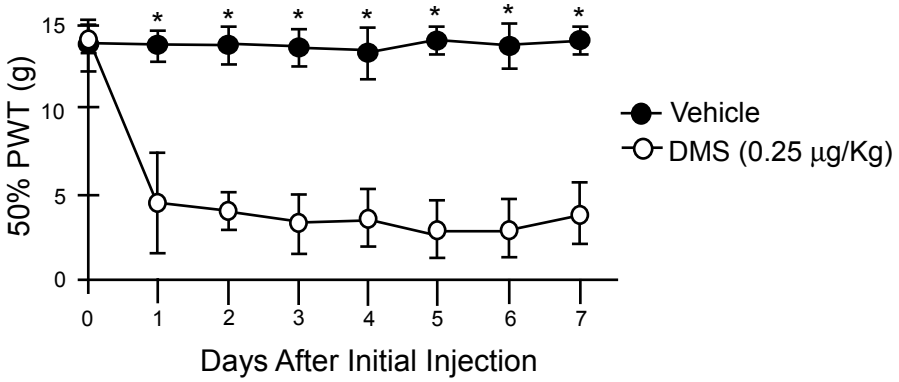

Supplementary Figure 13. Measurement of mechanical allodynia after intrathecal administration of DMS or vehicle. Measurements of mechanical allodynia on days of DMS administration were made prior to DMS injection. DMS was injected on days 0, 1, 2, 5, and 6. Measurements are expressed as 50% paw withdrawal threshold of mean ±SD. DMS was administered at a concentration of 0.25 μg/Kg and treated animals ($n=7$) showed a significant decrease in 50% paw withdrawal threshold (PWT) compared to vehicle controls ($n=6$) by a Student's t-test for unpaired data ($p<0.05$).

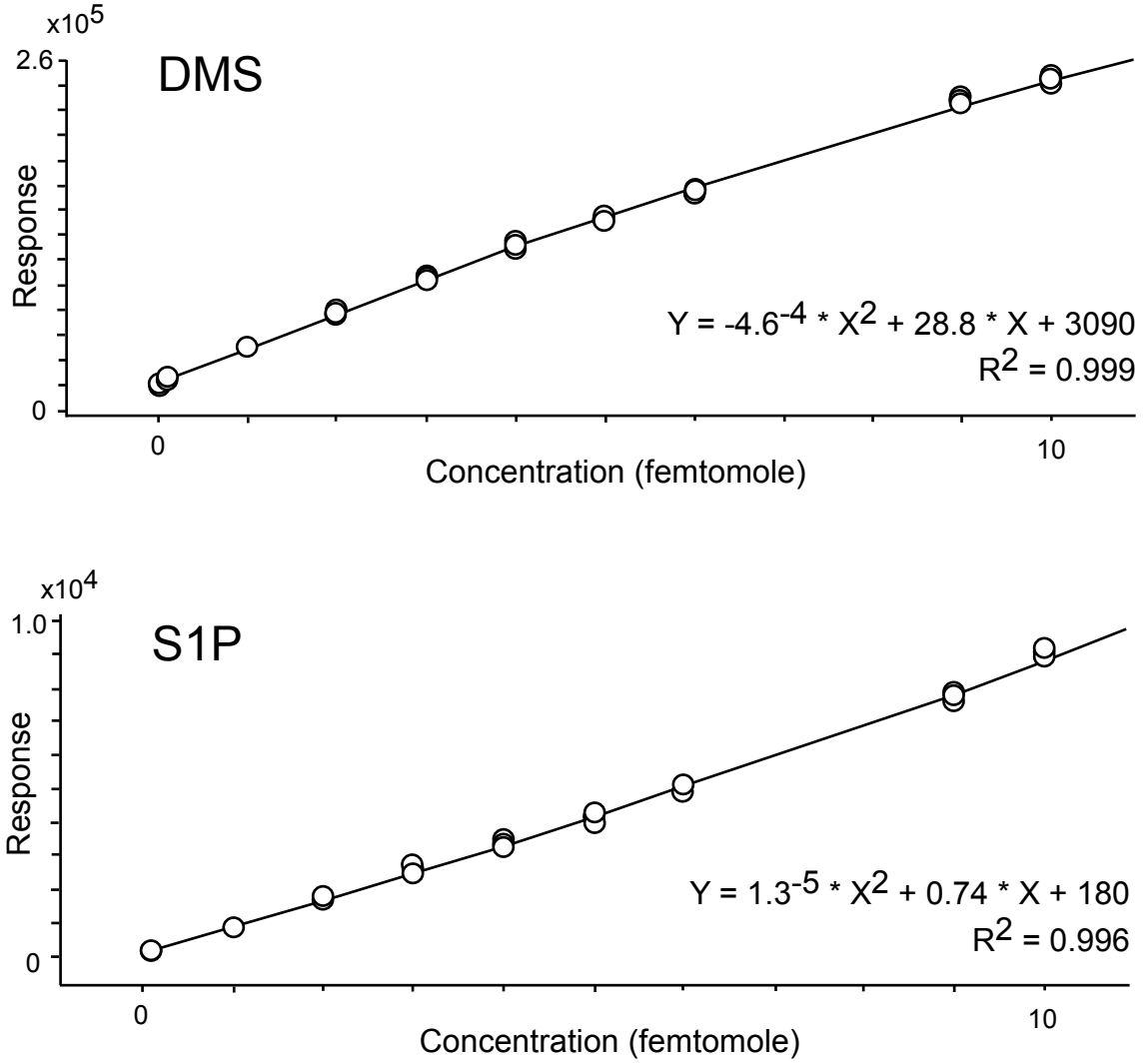

Supplementary Figure 14. Standard curves for DMS and S1P. Curves were constructed by using QqQ mass spectrometry. Data points from three experimental replicates are shown. Ion responses were determined by integrating quantifier ion transitions (listed in methods) for the standard dilutions shown.

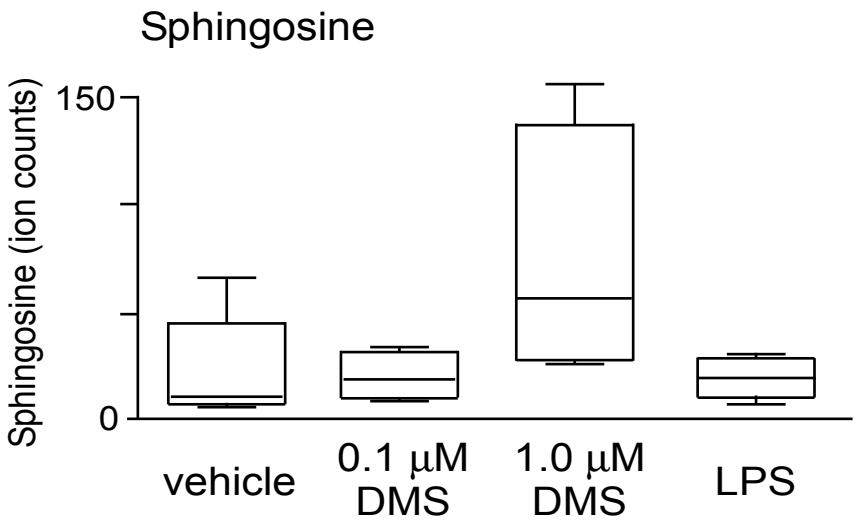

Supplementary Figure 15. Sphingosine levels in cultured astrocytes after DMS treatment. Sphingosine levels were measured by selective reaction monitoring by using the quantifier transition of *m/z* 300.3→282.3 and the qualifier ion transition of *m/z* 300.3→55.4. Treatment of astrocytes with 0.1 μM and 1.0 μM DMS did not significantly alter intracellular sphingosine levels relative to vehicle and LPS ($p>0.05$, $n=3$ cultures per group).

References

1. Hofmann, H.A., De Vry, J., Siegling, A., Spreyer, P. & Denzer, D. Pharmacological sensitivity and gene expression analysis of the tibial nerve injury model of neuropathic pain. *Eur J Pharmacol* **470**, 17-25 (2003).
2. Bennett, G.J. & Xie, Y.K. A peripheral mononeuropathy in rat that produces disorders of pain sensation like those seen in man. *Pain* **33**, 87-107 (1988).
3. Dixon, W.J. Efficient analysis of experimental observations. *Annu Rev Pharmacol Toxicol* **20**, 441-462 (1980).
4. Yanes, O., *et al.* Metabolic oxidation regulates embryonic stem cell differentiation. *Nat Chem Biol* **6**, 411-417 (2010).
5. Yanes, O., Tautenhahn, R., Patti, G.J. & Siuzdak, G. Expanding coverage of the metabolome for global metabolite profiling. *Anal Chem* **83**, 2152-2161 (2011).
6. Want, E.J., *et al.* Solvent-dependent metabolite distribution, clustering, and protein extraction for serum profiling with mass spectrometry. *Anal Chem* **78**, 743-752 (2006).
7. Wikoff, W.R., Pendyala, G., Siuzdak, G. & Fox, H.S. Metabolomic analysis of the cerebrospinal fluid reveals changes in phospholipase expression in the CNS of SIV-infected macaques. *J Clin Invest* **118**, 2661-2669 (2008).
8. Smith, C.A., Want, E.J., O'Maille, G., Abagyan, R. & Siuzdak, G. XCMS: processing mass spectrometry data for metabolite profiling using nonlinear peak alignment, matching, and identification. *Anal Chem* **78**, 779-787 (2006).